

FRAGMENTATION OF THE STRUCTURE IN AI-BASED ALLOYS UPON HIGH SPEED EFFECT

I. G. Brodova¹, E.V. Shorokhov², A. N. Petrova¹, I. G. Shirinkina¹,
I.V. Minaev², I.N. Zhgilev² and A.V. Abramov²

¹Institute of Metal Physics, Ural Division, Russian Academy of Sciences,
18 S. Kovalevskaya St., Ekaterinburg, 620041, Russia,

²Russian Federal Nuclear Center - Zababakhin All-Russian Research Institute of Technical Physics, P.O.Box 245,
Snezhinsk 456770, Chelyabinsk Region, Russia

Received: December 02,2009

Abstract. Aluminum alloys have high potential as light structural materials. In this work light and electron microscopy and X-ray diffraction were used to study the structure and phase composition of deformed bulk samples from the Al-7075 and the Al-3003 alloys. Severe plastic deformation was carried out by the dynamic channel angular pressing (DCAP). In this method the rate of deforming materials is estimated to $10^3\text{-}10^5 \text{ s}^{-1}$. The finite element method was used to model the deformation process for samples when they moved through intersecting channels. Optimal process parameters to form the uniform structure in the samples were determined. The resulting data of this studying indicate that the formation of ultrafine-grain (UFG) structure is result from two mechanisms – a fragmentation in multicomponent Al alloys (Al-7075) and dynamic recrystallisation in low-alloyed alloys (Al-3003). Such different structure formation demonstrates a realization of two channels of elastic energy relaxation. Thus, DCAP method can be applied effectively for production UFG ($\langle D \rangle \sim 200\text{-}500 \text{ nm}$) bulk samples from industrial aluminum alloys with high hardness values (in 1.5 times higher than initial state) and high plasticity.

1. INTRODUCTION

Bulk nanostructured metals are currently considered to be promising structural and functional materials of new generation. Two basic approaches their production are noted to exist. One of them is compaction of initial nanopowders and another one is formation of nanostructures in bulk samples due to refinement of the crystalline structure under severe plastic deformation (SPD) [1]. It was shown, SPD-materials possess a number of unique properties, i.e. high strength (several times higher as

compared with large-grained analogues) in combination with good plasticity, low-temperature, and high-rate superplasticity, as well as cyclic and radiation resistance. In the known methods of severe plastic deformation the coarse-grained structure is usually transformed into the ultrafine-grained structure when the tested sample moves in the equipment with the velocity of some millimeters per second. The deformation rate constraints are directly associated with the applied equipment such as press-type machines, rollers, etc. The low-rate modes of severe plastic deformation have appeared

Corresponding author: I. G. Brodova, e-mail: brodova@imp.uran.ru

historically, and practically all present-day developments aimed to produce ultrafine-grained materials use this short range of velocities. Nowadays, efficiency improvement is the high-priority task for the follow-on development of the severe plastic deformation methods.

On the basis of the equal-channel angular pressing technique (ECAP) [2], the high-rate method of ultrafine-grained structure formation in metals was developed [3-6]. The feature of this method is that it allows great deformations in a material due to the use of pulsed energy sources, such as powder combustion gases, explosion products, and electromagnetic energy. This work provides results how this method was used to produce the ultrafine-grained structures in aluminum based Al-7075 and Al-3003 alloys. Examples of the high-rate deformation process modeling are provided.

2. EXPERIMENTAL MATERIALS AND PROCEDURES

Fig. 1 shows the principle of the DCAP. In the experiments, the gun accelerated samples up to the rate of several hundreds meters per second and then directed into the die. The die has two channels, equal in cross-sectional area, that intersect at a channel angle Φ of 90° and radius of an internal channel's crossing area R of 7 mm. In special experiments to determine an optimal pressing conditions for producing homogeneous fine structure the die with $\Phi = 110^\circ$ and $R=0$ mm was used. Samples with 16 mm in diameter and 65 mm in length were used for experimentation. The material was deformed at the strain rate of 10^4 – 10^5 s $^{-1}$, and the pressure in the region of channel intersection runs to 5–7 GPa. The characteristic time of the deformation process ranged from several hundreds of microseconds up to a millisecond. In experiments velocity of the Al-3003 alloy samples through the channels (V) was varied from 150 to 300 m s $^{-1}$, number of passes (N) though two channels were varied from 1 to 4. For the samples of the Al-7075 alloy $V=150$ m s $^{-1}$, $N=1$ –2.

Light and electron microscopy and X-rays diffraction were used to study the structure and phase composition of the bulk samples of Al-based alloys produced by DCAP. The size of structural fragments in the deformed samples was calculated from the electron-microscopy dark-field patterns taken using transmission electron microscopy (TEM; «JEM-200CX»). The size of intermetallic crystals was determined using of scanning electron microscopy (SEM; «Quanta-200»). Determinations of the lattice parameter and phase analysis of the Al matrix be-

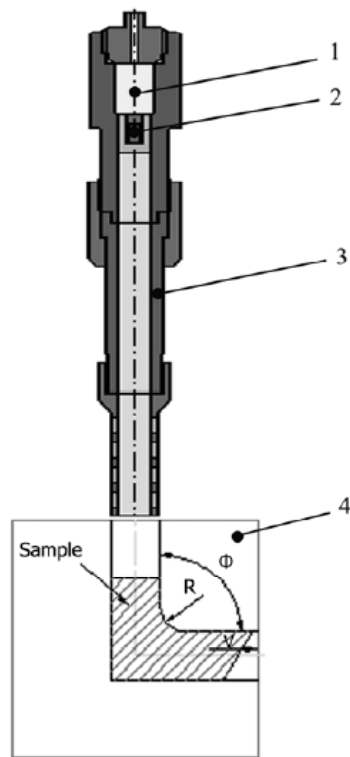


Fig. 1. Schematic of the dynamic deformation of a material: 1- powder charge, 2-sample, 3-barrel, 4 – matrix.

fore and after loading were performed with DRON-3 diffractometr in CoK α radiation. Analysis of the diffraction peak broadening of (331) α matrix reflection was used to determine the relative microdistortions of lattice for all samples. Vickers microhardness measurements were performed using PMT-3 device at 0.2 N load (the error does not exceed 10%). The microhardness was measured on the polished surfaces of the longitudinal and cross sections of all samples. For the calculation of the H_v the raw data were averaged from 10 values. Tensile tests of the Al 3003 alloy samples were carried out at room temperature with initial strain rate of 10^{-3} s $^{-1}$ on the ZWICK/Roell Z050 machine.

In order to study the structure and phase transformation by the heating of the Al-7075 alloy the samples after DCAP were subjected to thermal treatment according to two regimes.

First is double heating up to 120 and to 160 °C during 3 hours on each step. The second is the heating up to 200 °C during 1 hour.

Initial materials were rods of commercial multi-component Al-7075 and low-alloying Al-3003 alloys in hot-pressed and annealed states. They had a

banded polygonizide microstructure with subgrains of size 2 μm . The Al-7075 alloy (initial microhardness of the matrix is 680 MPa) is in a multiphase state and there are Al solid solution, isolated aluminides of manganese and iron, and the solid solution hardening MgZn₂ phase in the structure.

3. EXPERIMENTAL RESULTS AND DISCUSSION

3.1. Modeling of the deformation process

Numerical simulation of deformation of samples when they moved through the intersecting channels was performed using the finite element method in the program LS-DYNA. The task was to numerically calculate kinematical parameters of the sample and its stress-strain state in the process of loading, as well as residual strain of the sample and matrix and also to clarify how the internal and external angles in channels can influence the instantaneous characteristics of the sample.

Below the example of the problem solution for aluminum alloys is given. The statement of the problem was taken to be close to experiments. The dynamic deformation process was simulated on the Al-based alloy sample with the 16-mm diameter and the 65 mm length. The initial velocity of the sample reached 250 m s⁻¹. The number of finite elements is about 2000 items - to solve problems in the plane formulation, about 50000 elements - for solving problems in three-dimensional formulation. The calculation results in a flat statement in good agreement with the results of calculations in three-dimensional formulation for median cut sample.

For calculations the elastic plastic model of Johnson-Cook for aluminum alloy (1) was used. The equation of state (2) is in the Mie-Gruneisen form [7].

$$\sigma_y = (110 + 170\varepsilon_p^{0.36})(1 + 0.02 \ln \dot{\varepsilon}_p), \quad (1)$$

where σ_y - the yield stress, ε_p - plastic deformation, $\dot{\varepsilon}_p$ - rate of the plastic deformation.

$$P = \frac{\rho_0 C^2 \mu \left[1 + \left(1 - \frac{\gamma_0}{2} \right) \mu - \frac{a}{2} \mu^2 \right]}{1 - 0.339\mu} + (\gamma + a\mu)E, \quad (2)$$

where P - the pressure (hydrostatic),

$$\mu = \frac{\rho}{\rho_0} - 1,$$

$C=5383$ m/s - speed of sound, $\rho_0=0.0027$ g/mm³ - initial density of the material, ρ - current density of the material, $\gamma_0 = 1.97$ - constant, $a=0.48$ - constant.

It is assumed that the coefficient of friction depends on the relative velocity of contact surfaces

$$\mu = \mu_d + (\mu_s - \mu_d) e^{-d|v_{rel}|},$$

where $\mu_s=0.2$ - coefficient of static friction, $\mu_d=0.01$ - coefficient of dynamic friction, $d=0.6$ - coefficient of exponential decay, v_{rel} - relative velocity of contact surfaces.

The coefficients μ_d , μ_s , d were chosen by calculation and experimental, based on experiments where the samples were stranded in the matrix.

Fig. 2a gives the initial statement of the numerical experiment, and Figs. 2b, 3a, 3b give calcu-

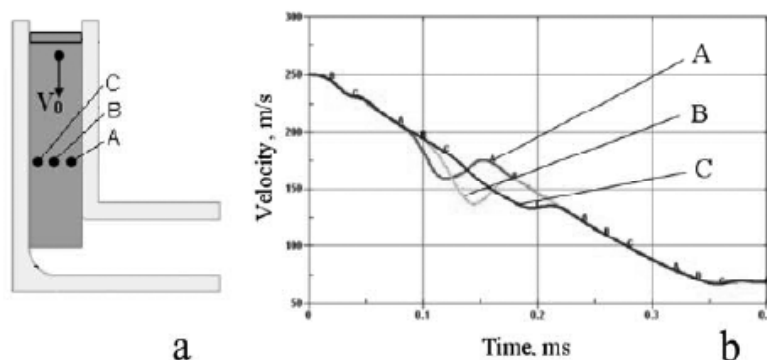


Fig. 2. Initial statement of the numerical experiment (a), velocities (b) test points on the sample.

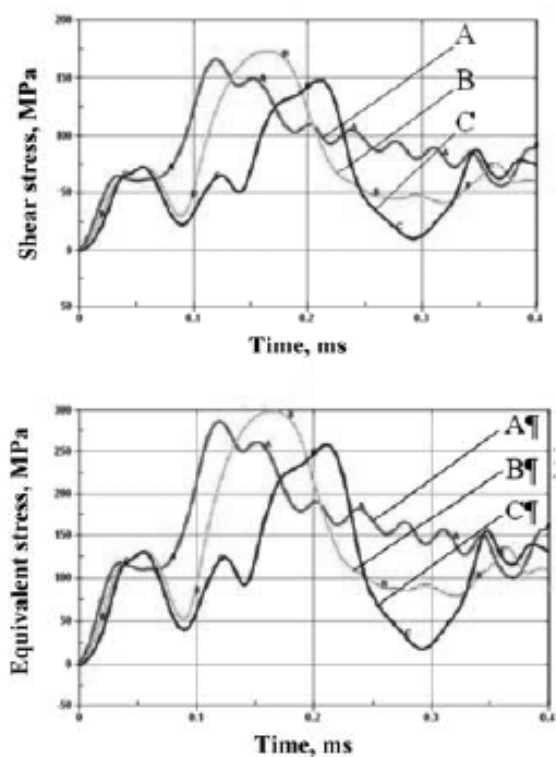


Fig. 3. Shear stress versus time (a) and Von Mises equivalent stress (b) in the area of test points on the sample.

lated velocities and stresses. These characteristics were determined for three random points in the middle cross section of the sample (Fig. 2a). Distribution of accumulated plastic deformations is presented in Figs. 4a, 4b.

Expectedly, the highest stress-and-deformation gradients arise in the place of channels intersection, since this is just the location where the quasi-stationary area of stress drop is formed. At that, velocities of different areas on the same cross-section of the sample are also different. Stress was observed to have the unsteady character in the area adjacent to the internal angle. Sample portions adjacent to the internal part of the channel turn out to be more stressed as compared to the internal part. On the whole, the stress-strain state of materials at certain instants of time is characterized by greater inhomogeneity.

Calculation results allowed a number of useful conclusions, in particular, that it is necessary to form the uniform structure in the sample. Our experiments demonstrated that this is possible by means of multiple and repeated loading of the sample. Variation of angle Φ showed the maximum deformation to be observed at $90-110^\circ$ angles. The bottom velocity threshold, that ensures the samples to pass through the channels, is comparatively low. For tested materials, this threshold velocity is $200-300 \text{ m s}^{-1}$ (without the external pressure). The matrix retains its elastic state within a wide range of velocities and this allows its multiple re-use.

3.2. Structure and phase transformation of the Al-7075alloy

Fig. 5a shows the typical structure of this alloy after one pass DCAP with $V=150 \text{ m s}^{-1}$ ($\Phi=90^\circ$, $R=7 \text{ mm}$). According to TEM images the characteristics of this deformed state are high dislocation density,

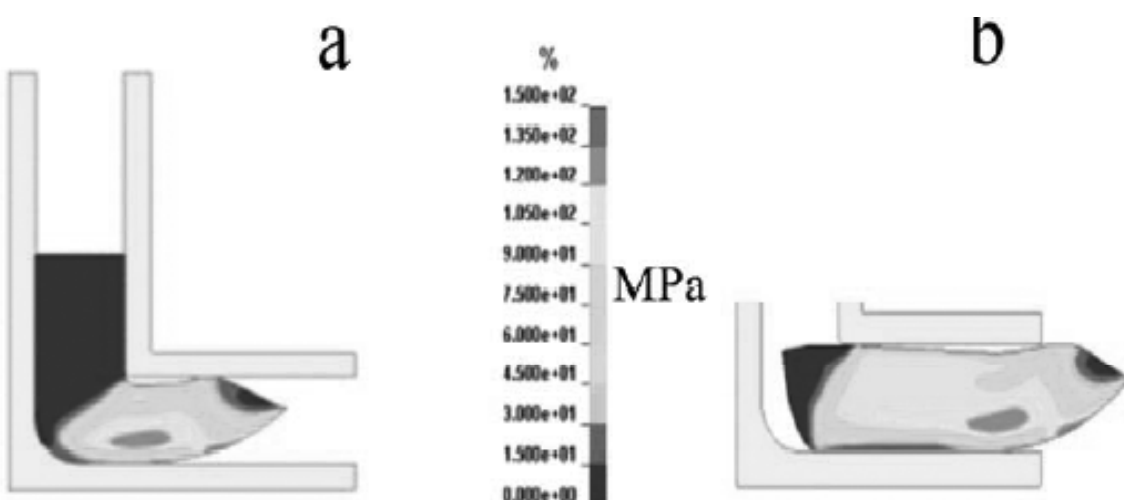


Fig. 4. Distribution of accumulated plastic deformations in the sample at the moment corresponding to half length passage (a) and complete passage of the sample (b).

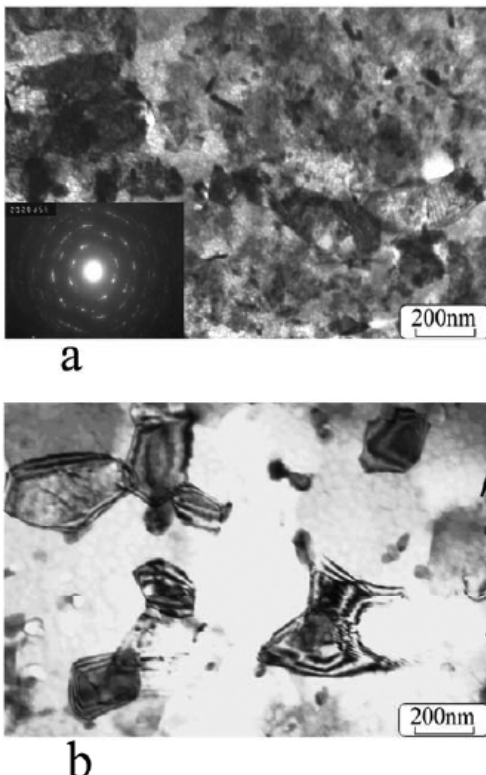


Fig. 5. TEM images of Al 7075 alloy structure after DCAP ($N=1$, $\Phi=90^\circ$, $R=0$ mm, $V=150$ m s $^{-1}$) (a), and after DCAP and double heating ($N=1$, $\Phi=90^\circ$, $R=0$ mm, $V=150$ m s $^{-1}$) (b).

wide high-angle boundaries between structure fragments with inhomogeneous internal contrast. Structural-phase state of the sample becomes more non-equilibrium after the second pass (route B_c in which the sample rotated by 90° in the same direction between each pass). Calculating of average size of crystallites was carried out from dark field electronic microscope pictures. Size distribution histogram of crystallites in the structure of one-pass sample was built and shows that average size is 200 nm (Fig. 6). The basic share ($n=60\%$) is structure elements are less than 200 nm in diameter, but there are individual fragments more than 500 nm in size. With increasing DCAP passes the area fraction of coarse grains and their size decreased, however the average grain size was remained above 180-200 nm.

To determine the changes in the stressed state of material and the degree of strain hardening of the matrix after DCAP the lattice microdistortions were estimated. We calculated microdistortions of the

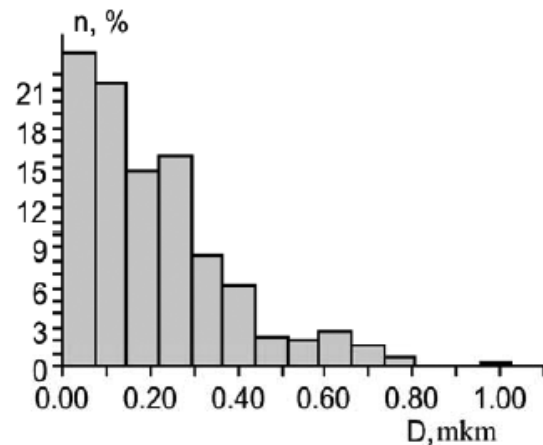


Fig. 6. Size distribution histogram of crystallites in the deformed sample ($N=1$). Where n is quantitative share of crystallites with average size D .

matrix lattice according to the relative change in the X-ray half-width of line of specimens. Fig. 7 illustrates the changes in the peak profile of the (331) α Bragg reflection depending on number of passes in comparison with initial state. Observed decreasing of intensity and increasing of integral width of (331) α Al peak profiles of deformed samples, can be explained by a growth of internal microstresses and, correspondently, by a large lattice microdistortions. Therefore, inhomogeneous structure of the Al-7075 alloy is formed on dislocation mechanism mainly as a result of cold work. So, the relaxation of elastic energy upon DCAP of samples carried out by plastic deformation, due to the fragmentation of subgrains of initial structure.

To study the features of phase transformation taken place during deformation of high-alloyed Al-7075 alloy electronic microscopy and X-rays diffraction methods were used.

The results showed that the alloy remains in a multiphase state after deformation. From analysis of diffraction patterns taken from the initial and deformed samples, it should be established that phases which partially preserved in the process of deformation are isolated aluminides of manganese and iron, and the solid solution hardening MgZn₂ phase. According to SEM, number of the MgZn₂ intermetallics reduced and their size decreases from 300 to 5-10 nm. This may serve as proof of their partial deformation dissolution in the process of DCAP. Additional alloying of the matrix leads to a change in the lattice parameter, it decreases from 0.4054 to 0.4052 nm. Since zinc reduces the lat-

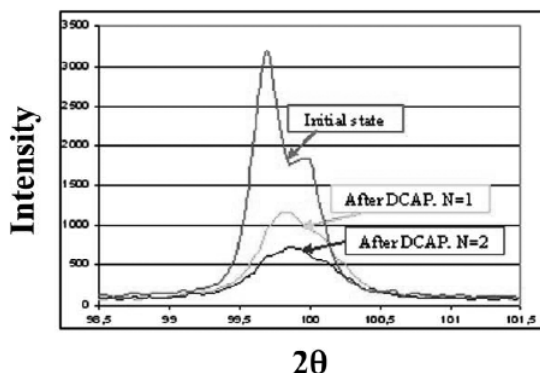


Fig. 7. Peak profile of the (331) Bragg reflections transformation depending on passes.

tice parameter of aluminum and magnesium increases it, it is difficult to assess the degree of supersaturation of solid solution by these elements. But the fact of change in the lattice parameter of aluminum can also serve as proof of an additional alloying of the matrix and an increase in solid-solution hardening. Remained in the structure after pressing intermetallic particles basically situated on crystals boundaries and their size (5-10 nm) provides sufficient barrier effect for UFG structure stabilization (Fig. 5a).

The formation of UFG structure affects on material hardness. The total strengthening effect of material during DCAP caused by the above factors (UFG structure, supersaturated Al solid solution, dispersed aluminides and structure defects) can be illustrated by a change of microhardness. It was established that after deformation H_v increases by a factor of 1.5 in comparison with initial state. In special experiments the influence of channel geometry on the value and behavior of the distribution of microhardness over the cross-section of the deformed specimens was investigated. In particular, when $\Phi=90^\circ$ and $R=7$ mm surface layers of 2 mm thick have the hardness on 200-250 MPa higher than the center. At this geometry value H_v in the center of the sample after one pass is 1100 MPa. Two-pass sample has the same H_v in the center, but the dispersion of average values of the cross section is smaller (100-150 MPa). Increasing the angle of intersection of channels Φ to 110° ($R=7$ mm) lowers the H_v to 950 MPa. The smallest dispersion of average values of the microhardness over the cross section is observed at $\Phi=90^\circ$ and $R=0$ mm.

Different values of H_v in the cross section of the sample confirm the mathematics estimate of the heterogeneity of the stress-strain state at different points in the sample. Some fluctuations in the values of H_v of the samples obtained at different geometries of the channels associated with the change in the value of strain hardening, which occurs due to different plastic deformation in the shear plane.

The thermal stability is very important factor of formed UFG structure. It regulates by phase transformations such as an ageing and a recrystallisation. Considering that additional alloying of Al solid solution accompanies severe plastic deformation, it was necessary to find out the sequence of these processes and their features. To study these phenomena the samples of Al-7075 alloy were heated by two regimes. First is double heating up to 120 °C and to 160 °C during 3 hours on each step. The second is the heating up to 200 °C during 1 hour.

According to SEM and X-ray diffraction data the main phases after all regimes of heat treatments are the Al solid solution and the MgZn₂ crystallites. The TEM data showed that an ageing process with a precipitation of supersaturated solid solution and formation of the MgZn₂ strengthening phase takes place only during double heating. In this, the lattice parameter increases and after the heat treatment is 0.4059 nm, what also shows the precipitation of intermetallides from the Al solid solution.

Simultaneously with ageing there is recovery process during heating of deformed samples, which leads to the formation of more equilibrium boundaries and removes the strain work hardening (Fig. 5b). As a result of combined phase and structural transformations dispersed two-phase structure was formed. It consists of the Al matrix grains, separated by equilibrium boundaries, and strengthening MgZn₂ phase, located both on the boundaries and inside the grains. These intermetallides play the role of an additional barrier to the growth of grains of the matrix, and contribute to the preservation of their small size achieved upon DCAP. Changes in the structure of the material during heating cause a corresponding change to its hardness, namely, it decreases due to relaxation of internal stresses and increases due to dispersion hardening. Measurements showed that the hardness of the material after two-steps aging is equal 1000 MPa, and the superposition of two processes leads to the preservation of high values of hardness, in 1.5 times higher than the original. Thus, the first regime of heat treatment of DCAP samples stabilizes UFG structure and retains its high strength.

Heat treatment of the second regime leads to a slight increase in the average grain size of 300 nm. The probable cause of this grain growth is the “purification” of the boundaries because of the dissolution of disperse $MgZn_2$ particles and the beginning of the recrystallization process.

3.3. Structure and phase transformation of the Al-3003 alloy

In the Al-3003 alloy (initial microhardness of the matrix – 480 MPa) in the same modes DCAP a different picture is observed. Formation UFG structure with grain size of ~ 350-400 nm occurs in several ways [8]. At $N \leq 2$ and $V \leq 300 \text{ m s}^{-1}$ a mixed structure characterized by a high density of dislocations within the fragments, separated by diffuse high-angle boundaries, a presence of subgrains with low-angle misorientation is produced.

Evolution of the stress state, drawn from the X-ray line profile analysis of Al matrix, indicates the emergence of high fields of internal stresses. Such an inhomogeneous structure is formed on dislocation mechanism mainly as a result of cold work.

With an increase in $N \geq 4$ and $V \geq 300 \text{ m s}^{-1}$, the grains become free of dislocations, and high-angle equilibrium boundaries with well distinguishable extinction contours are formed; i.e., the observed structural changes indicate the relaxation of the strained lattice state. According to TEM data the average size of the structure fragments slightly depends on V and to obtain the structure with the scale of less than 400 nm is not possible at all investigated modes of deformation of this alloy.

The observed structural states are confirmed by data on the hardness. The hardness values for the samples obtained at $N \leq 2$ and $V \leq 300 \text{ m s}^{-1}$ is less than the initial hardness on 500 MPa, while for samples at $N \geq 4$ and $V \geq 300 \text{ m s}^{-1}$ on 300 MPa. Because the average size of the fragments of the structure doesn't depend on V , we can assume that the hardness reduces due to the removal of cold hardening and transition of the material in a state of equilibrium [9]. These data allow to conclude that the formation mechanism of UFG structure depends on DCAP conditions. It was found that at $V \leq 150 \text{ m s}^{-1}$ and $N \leq 2$ relaxation of elastic energy is carried out by plastic deformation, due to the fragmentation of 2 mkm subgrains of the initial structure. When $V \geq 300 \text{ m s}^{-1}$ and $N \geq 4$ the deformation is accompanied by intensive dynamic recrystallization, as one of known channels of elastic energy dissipation [10]. These results demonstrate the cyclicity of structural transformations with increasing of degree of

the deformation and the implementation of two channels of relaxation of elastic energy during DCAP of the Al-3003 alloy.

Formation of UFG structure in the bulk samples had a positive effect on their mechanical properties. Thus, for Al-3003 alloy tensile stress value increases in 1.5 times compared with hot-pressed condition, reaching the value σ_B as after cold working but keeping high value of plasticity ($\delta=13\%$) as in annealing state.

4. CONCLUSIONS

The method of plastic severe deformation – DCAP can be used effectively for producing ultrafine-grain ($<D>\sim 200\text{-}500 \text{ nm}$) bulk samples from industrial aluminum alloys. Optimal process parameters (velocity V of the samples motion through the channels and the number of passes) were determined. There are $V=150\text{-}300 \text{ m s}^{-1}$, $N=1\text{-}4$. ($\Phi=90^\circ$, $R=0 \text{ mm}$).

Scale of UFG structure depends on the alloy composition. When the alloying degree of the Al-solid solution and solid-solution hardening of the initial state are more higher, then the fragments of the deformed structure are smaller. Grain size of the structure is 200 nm in the Al-7075 alloy with initial base microhardness of 680 MPa. This parameter is twice smaller in the Al-3003 alloy with an initial hardness of 480 MPa.

The results indicate that the formation of UFG structure in commercial Al alloys can be the result of two processes – a fragmentation in multicomponent Al alloys and dynamic recrystallisation in low-alloyed alloys. It is established the hardness of the materials increases in 1.5 times after DCAP. The tensile strength of the Al-3003 alloy after DCAP increases by a factor of 1.5, reaching the one after cold hardening, and high plasticity is as in annealing state.

High DCAP productivity caused by absence of expensive equipment, short deformation process time and opportunity to produce ultrafine-grain structure in big bulk samples by less passes compared to ECAP was proved.

ACKNOWLEDGEMENTS

This work was supported by Russian Foundation of Basis Researcher (grant № 08-03-00106) and the Program of the Presidium of the Russian Academy of Sciences “Heat physics and mechanics of extreme energy effects and physics of high compressed substance”.

REFERENCES

- [1] R.Z. Valiev and I.V. Alexandrov // *M. IKTs «Akademkniga»* (2007) 397.
- [2] V.M. Segal, V.I. Reznikov and A.E. Drobyshevskii // *Metals.* **1** (1981) 115.
- [3] E.V. Shorokhov, I.N. Zhgilev and R.Z. Valiev // *Patent No. 2 283 717* (2006).
- [4] E.V. Shorokhov, I.N. Zhgilev and D.V. Gunderov // *Phys. Chem. B* **2** (2008) 251.
- [5] V.I. Zeldovich, E.V. Shorokhov and N.Yu. Frolova // *Fiz. Met. Metalloved.* **105** (2008) 431, In Russian.
- [6] I.V. Khomskaya, V.I. Zeldovich and E.V. Shorokhov // *Fiz. Met. Metalloved.* **105** (2008) 621, In Russian.
- [7] G.R. Johnson and W.H. Cook, *Proceedings of the 7-th Internationals Symposium on Ballistics* (The Hague, The Netherlands, 1983), 541.
- [8] I. G. Brodova, I. G. Shirinkina, O. A. Antonova, E. V. Shorokhov and I. I. Zhgilev // *Materials Science and Engineering A* **503** (2009) 103.
- [9] I.G. Brodova, I. G. Shirinkina, T. I. Yablonskikh, V. V. Astaf'ev, E. V. Shorokhov and I. N. Zhgilev // *Bulletin of the Russian Academy of Sciences: Physics* **73** (2009) 1257.
- [10] A.M. Glezer // *Izv. Ross. Akad. Nauk, Ser. Fiz.* **71** (2007) 1764.

